Increased Fracture Toughness of Graphite-Epoxy Composites through Intermittent Interlaminar Bonding

LI- CHUNG JEA AND DAVID K. FELBECK

Department of Mechanical Engineering
University of Michigan
Ann Arbor, Michigan 48109

ABSTRACT

The objective of this study has been to increase the fracture toughness of multi-layer continuous-filament graphite-epoxy composites. The method used is intermittent interlaminar bonding, which can lead to a large increase in the fracture surface area. In this study we achieved intermittent bonding through introduction of thin perforated Mylar between the layers of the composite. For the best optimum condition included in this study, fracture toughness was increased from about 100 kJ/m² for untreated specimens to an average of about 500 kJ/m², while tensile strength dropped from 500 MPa to 400 MPa, and elastic modulus remained the same at about 75 GPa. An approximate analysis is presented to explain the observed improvement in toughness.

INTRODUCTION

LOW FRACTURE TOUGHNESS is a deficiency of high strength high modulus fiber reinforced composites [1]. One method for alleviating this deficiency in boron-epoxy composites has developed through techniques for altering the characteristics of the filament-matrix interface [2, 3]. However, reducing the interfacial bonding between filament and matrix is a tedious and expensive job, so a more practical technique for increasing fracture toughness, through altering the bonding between layers of prepreg tape, was developed and tested. This paper describes the experimental results of application of these techniques to cross-ply graphite-epoxy composites.

The bond between adjacent layers of a composite made of laid-up prepreg layers is normally controlled by the strength of the matrix, in this case a high-strength

epoxy. Any interface is thus effectively eliminated during curing of the composite, and a crack initiating in one region can readily propagate transversely into adjacent layers. The technique that we have used for producing intermittent bonding between layers consists of interspersing a perforated layer of 7-μm thick Mylar between adjacent layers of prepreg tape as it is being laid up, prior to curing. The perforation consists of a matrix of holes, in most cases about 1 mm diameter. Thus the hole fraction of the total contact area represents the fraction of strong bonding between adjacent layers, while the remaining Mylar leads to relatively low-strength bonding.

Intermittent interlaminar bonding enhances the fracture toughness of the composite laminates by blunting and diverting the internal crack of one lamina, usually caused by fracture of a filament. As shown in Fig. 1, if the fracture strength at the point on the interface where the crack first emerges happens to be low, interlaminar subcracking occurs and blunts the crack front. This prevents the low ductility filament fracture from initiating catastrophic failure. If the interface strength first met by the crack is high, the fracture may run through the next layer along a fraction of its length but will be effectively halted along those portions of its length that have low interface strength.

The intermittent bond type of composite will also maintain the strength and stiffness of the laminate even though the total energy required for fracture may increase. Triaxiality of stress leads to formation and propagation of an interlaminar subcrack in the weak-bond region as shown in Fig. 2. The energy required to fracture the strong-bonded interface in the treated laminate eliminates premature complete delamination under tensile load in an unnotched laminate and this maintains the strength of the composite.

In terms of work of fracture, an intermittently bonded interface in a cross-ply composite provides the conditions that encourage the interlaminar subcrack to propagate. As shown in Fig. 3, when a through crack in a laminate reaches the weak bond region the induced lateral stress will open up the weak interface. If the crack propagation resistance is different for each layer (for example, in adjacent plies with filaments at different angles) the crack will propagate further in one layer than the others. Consider two adjacent plies as shown in Fig. 3a where the crack in ply 2 is longer than in ply 1. Lateral contraction at the tip of ply 2 plus the longitudinal displacement of the fracture surfaces of ply 2 following fracture leads to creation of a longitudinal interlaminar subcrack ahead of the crack in ply 1 [4], Fig. 3b. Cook and Gordon [5] state that the tensile strength of the weak bond region must be less than one-fifth of the cohesive strength of the interface to enhance the mode I type of debonding at the crack front.

EXPERIMENTAL TECHNIQUE

Prepreg tape, manufactured by Narmco Materials Incorporated (sold as Rigidite 5208/T300 prepreg tape), was cut and stacked (usually 8 or 9 layers) in its desired

LOAD

CARBON FILAMENTS

STRONG BOND INTERFACE

WEAK BOND INTERFACE

INITIATING CRACK IN FILAMENT

BLUNTED INTERLAMINAR CRACK

THICKNESS OF ONE LAMINA

LOAD
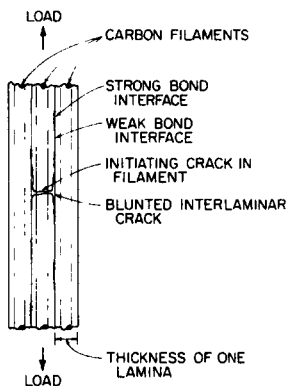
Figure 1. Blunting mechanism of a crack originating in one layer of a composite.

LOAD

INTERLAMINAR SUBCRACK SHOWN IN (b)

PLANE OF TRANSVERSE CRACK

LOAD

HOLES IN INTERLAMINAR MYLAR (CONTACT REGION)

SUBCRACK FRONT

STRONG BOND REGION

WEAK BOND REGION (CRACKED)

SUBCRACK DIRECTION
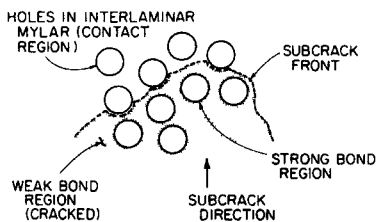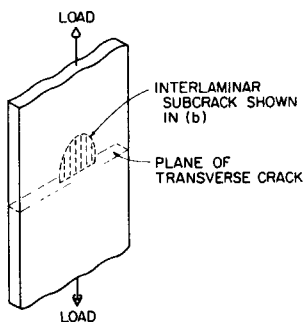
Figure 2. Subcrack propagation in the intermittently bonded interface.
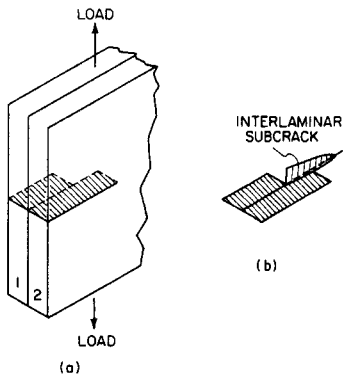
LOAD

INTERLAMINAR SUBCRACK

(b)

Figure 3. Interlaminar subcrack resulting from different crack growth rates in adjacent plies. a) Initial transverse cracks. b) Resulting interlaminar subcrack that occurs between plies 1 and 2.

1
2

LOAD

(a)

247

configuration, with or without interlaminar Mylar (7 μm thick), with or without holes, and placed in a steel mold. We used prepreg tape manufactured in 1976 and 1978, purchased to the same specification, but some differences were observed as are noted with the test results below. When a lay-up of $\phi, \phi, \phi, -\phi, \ldots$, is used (see definition of symbols at end of paper), $\alpha = \phi$ and $\beta = 2\phi$; this special geometry is called "angle ply".

A layer of 7-μm thick Mylar containing an array of fine holes was used to vary the amount (percent) of contact area between plies of tapes. Zero percent contact occurs when Mylar without holes is used; 100% contact occurs when no Mylar is used.

The specimens were cured in a Blue M #POM-18VC-2 vacuum oven at 180°C for 3 h (10.8 ks) with a dead load pressure of 10.8 kPa. A reinforced modified compact tension specimen was used for the fracture toughness tests, Fig. 4, and dumb-bell shaped specimens were used to evaluate the elastic modulus and tensile strength of the composites, Fig. 5. Tests were conducted on either a 4.9-kN Instron Universal Testing Machine or a 45-kN Instron Universal Testing Machine, depending upon the maximum load needed to perform the test.

The Gurney sector-area method was used to measure the fracture toughness of each specimen [6]. The details of the experimental procedure are described in references [7, 8].

TEST RESULTS

Tensile Test Results

Eight-layer angle ply $(\phi/-\phi/\phi/-\phi/\phi/-\phi/\phi/-\phi)$ and 8- or 9-layer quasi-isotropic structured laminates, laminates having similar in-plane properties in every direction, and some 3-layer laminates were tested to obtain the elastic modulus and tensile strength of the material. Figure 6 shows that the elastic modulus of the material decreases monotonically as $\alpha+\beta$ increases.

Tensile strength of 8-layer angle-ply laminates is also plotted with respect to the value of $(\alpha+\beta)$ in Figs. 7 and 8. The average filament volume fraction of the 1976 batch was 61%, and the areal fiber weight was 157 g/m². The average filament volume fraction of the 1978 batch was 58%, and the areal fiber weight was 155 g/m². We are not aware of any other differences between those two batches.

Owing to the edge effect, our experiments suggest that for angle-ply laminates in all except very small lay-up angles, the tensile strength is actually a measure of the interlaminar shear strength. The edge effect is illustrated by Fig. 9. Here an 8-layer angle-ply tensile specimen with 18% contact and $\phi = 15°$ is shown. No fracture of the filaments is detectable in this picture.

Fracture Toughness Test Results

As a first approximation the value of the sum of α and β is used to describe the

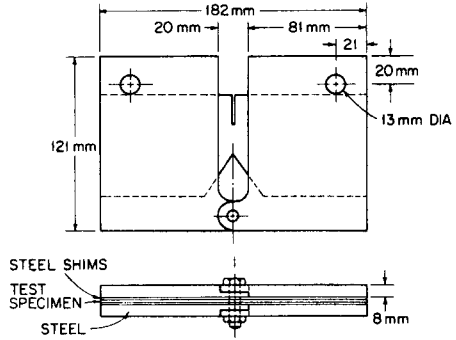*Figure 4. Reinforced modified compact tension specimen for measuring fracture toughness.*

Figure 5. Dumb-bell specimen for measuring tensile strength and e-lastic modulus.
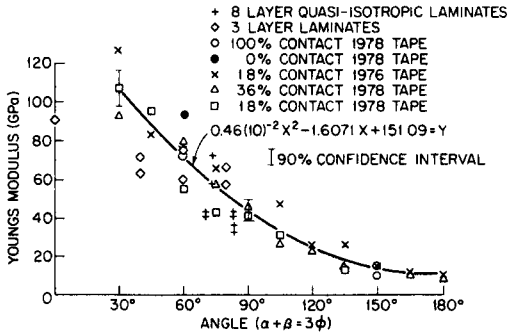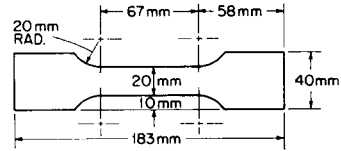

+ 8 LAYER QUASI-ISOTROPIC LAMINATES
◇ 3 LAYER LAMINATES
○ 100% CONTACT 1978 TAPE
● 0% CONTACT 1978 TAPE
× 18% CONTACT 1976 TAPE
△ 36% CONTACT 1978 TAPE
□ 18% CONTACT 1978 TAPE

$0.46(10)^{-2}X^2 - 1.6071\,X + 151\,09 = Y$

I 90% CONFIDENCE INTERVAL

Figure 6. Elastic modulus of all 8-layer angle-ply laminates.

249
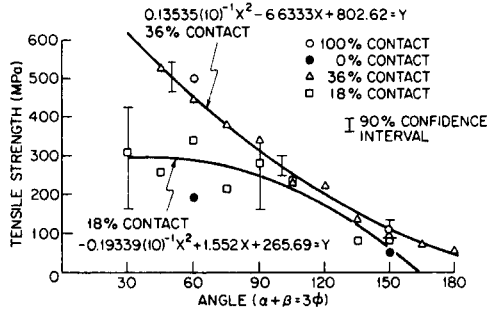
Figure 7. Tensile strength of 8-layer angle-ply laminates (made of 1978 prepreg tape), for 18% and 36% contact.
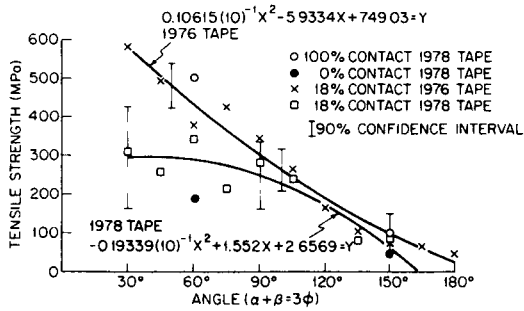

Figure 8. Tensile strength of 8-layer angle-ply laminates (made of 1976 and 1978 prepreg tape), for 18% contact.
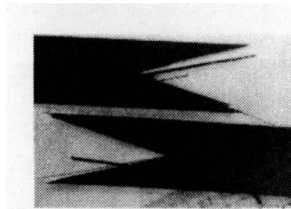

Figure 9. *18% contact, $\phi = 15°$ dumb-bell specimen after fracture: tensile strength is 494 MPa, elastic modulus is 83 GPa, all plies delaminated.*

essential geometry. The parameter $\alpha+\beta$ is a measure of the orientation of the filaments to the loading direction, α, and the angle between adjacent filament layers, β. The fracture mode should in part thus be controlled by $\alpha+\beta$. The observed average delamination length of the laminae (measured parallel to the loading direction), which is proportional to the delamination fracture area, is plotted as a function of the sum of α and β in Fig. 10. For 36% contact specimens, the observed pull-out length increases with α and β. For 18% contact laminates, specimens made from both 1976 batch tape and 1978 batch tape show a local minimum in the pull-out length at $\alpha+\beta$ equal to 90° and 120° respectively.

The work of fracture values vs. $\alpha+\beta$ for 8-layer angle-ply and 8- or 9-layer quasi-isotropic specimens have also been plotted in Figs. 11–14. Polynominal equation curves best fitting the test results based on lease square analysis are also presented. For each particular curve 90% confidence intervals for $\alpha+\beta$ equal to certain key values were calculated and inserted at the corresponding places.

In Fig. 11, data from specimens made of both 1976 batch tape and 1978 batch tape are compared. Both data sets show double-humped curves. The peak that occurs at $\alpha + \beta \approx 60°$ corresponds to the high point C of Fig. 10 and the low point at $\alpha + \beta \approx 100°$ corresponds to point B of Fig. 10.

Figure 12 has incorporated all the test data for specimens of 8-layer quasi-isotropic laminates with interfacial bond treatment. All the data points still fit a double-humped curve similar to Fig. 11.

Figure 13 shows test data for 36% contact specimens. The toughness is low when $\alpha+\beta$ is less than 90°. When $\alpha+\beta$ becomes larger than 90°, the work of fracture increases and reaches a maximum at $\alpha + \beta = 150°$ and then drops for larger angles.

Toughness of 100% contact laminates is plotted in Fig. 14 as a comparison. Scattered data with a maximum value of 299 kJ/m^2 can be seen. No particular correlation between the fracture toughness and $\alpha+\beta$ was observed.

ANALYSIS AND DISCUSSION

Strength

The interlaminar fracture mode exhibited by Fig. 9 is shown in its simplest form for a 2-ply specimen in Fig. 15a. As shown in Fig. 15b the length L times the width w is proportional to the area of the effective contact surface between two adjacent plies. Since $L = w \cot \phi$, $(w^2 \cot\phi)/2$ is then the nominal interlaminar surface fracture area. Besides the interfacial bonding, the in-plane crack area of a lamina also plays a role in the tensile strength. By assuming the operation of the same mechanism to fracture the bond (either in shear or in tension) we can simplify the situation by considering only the total interlaminar surface fracture area A involved.

$$A \propto \cot \phi$$

251

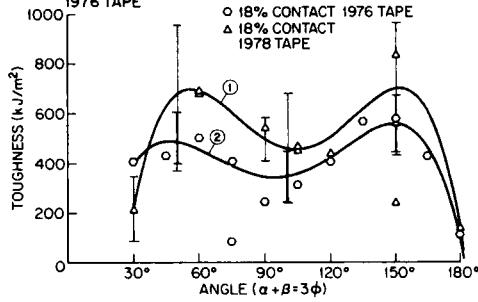Figure 10. Average delamination length as a function of α+β for 8-layer angle-ply laminates.
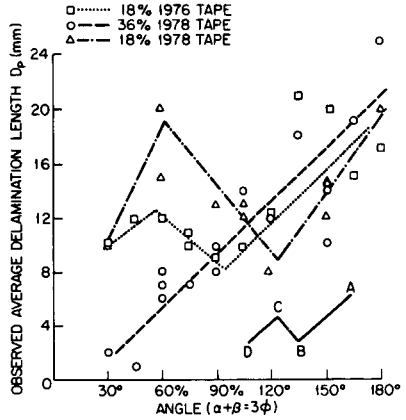
Figure 11. Fracture toughness as a function of α+β for 8-layer 18% contact angle–ply laminates made from 1976 and 1978 tape.
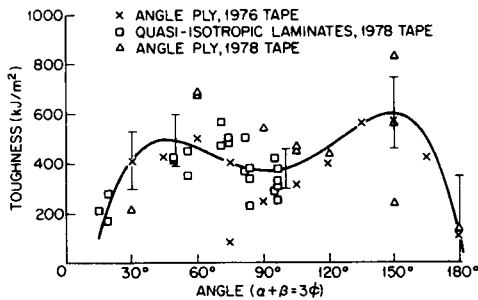

Figure 12. Fracture toughness as a function of α+β for 8-layer 18% contact quasi-isotropic laminates made from 1978 tape, combined with data of Fig. 11.

$Y = -0.88356(10)^{-6}X^4 - 0.37371(10)^{-3}X^3 + 0.14778X^2 - 6.2558X + 75.96$
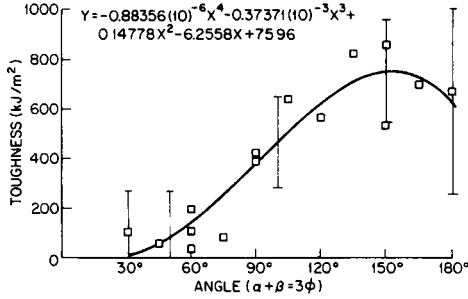
Figure 13. Fracture toughness as a function of α+β for 36% contact angle-ply laminates.

× 8-LAYER ANGLE PLY LAMINATES
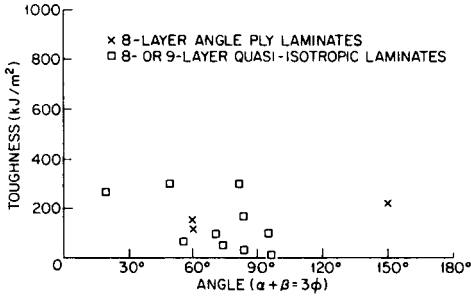□ 8- OR 9-LAYER QUASI-ISOTROPIC LAMINATES

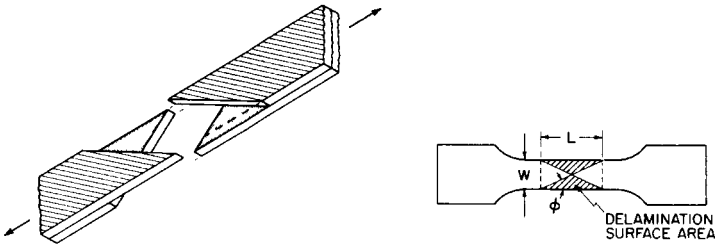*Figure 14. Fracture toughness for 100% contact laminates.*

Figure 15. Contact surfaces and shear stress of an angle-ply laminate.

253

The strength S can then be given as:

$$S = K \cot \phi$$

Based upon a tensile strength of $S = 75$ MPa when $\alpha + \beta = 180°$, $\phi = 60°$, K was found to be 130 MPa. A curve for $S = 130$ MPa cot ϕ is drawn for comparison with the tensile strength data of angle-ply laminates in Fig. 16. We conclude that the interlaminar surface fracture area dominates the tensile test and the interlaminar shear stress thus determines the strength of a narrow cross-ply composite.

Fracture Modes

Figure 9 shows the appearance of simple, complete delamination that can occur without any filament fracture. In real fracture toughness tests, the fracture surface that results in a 2-ply laminate, shown in exaggerated thickness, appears as in Fig. 17. The average delamination length, D_p, shown in Fig. 10 is basically half of the total delamination zone size.

While the test results to date do not lead to a clear explanation of the influence of the several variables involved, one possible qualitative approach may be helpful. Specimens with large $\alpha+\beta$ angles that correspond to the region A-B in Fig. 10 show decreasing delamination size as ϕ decreases. This is attributed to having a larger delamination tendency when angle β increases. In region B-C, for 18% contact specimens, the raising of the required crack extension force to propagate the gross crack across the filaments as α becomes smaller, in addition to the force for delamination energy, leads to an increase in average pull-out length. In region C-D, the curve drops again, and it may be argued that as β becomes smaller, the energy allocated to delamination in fracturing becomes small compared to the energy allocated to propagate the gross crack across the filaments, and as β becomes smaller the delamination area diminishes rapidly so that the average pull-out length becomes very small. This last argument can also be supported by the load-displacement plots for the fracture toughness test in which instability, sudden fracture from a high load, always occurs with specimens of small α angle.

There are two major differences between 36% contact interface and 18% contact interface. First is the difference in the interlaminar cracking speeds. In 36% interfacial contact specimens, the delamination speed is slower, or in other words, delamination toughness is higher. Secondly, in 36% interfacial contact specimens, the direct contact between plies is higher than that of the 18% contact specimens. Thus cracks in 36% contact specimens have more chances to propagate through the thickness of the whole laminate without being blunted by the weak bond regions at the interface. For the aforementioned two reasons, the gross transverse crack is easier to propagate and interlaminar cracks are more difficult to propagate in 36% contact specimens compared to 18% contact specimens in the small $\alpha+\beta$ angle region. Thus the increase in average pull-out length that occurs in 18% contact
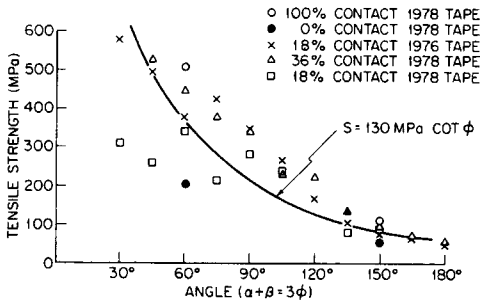
Figure 16. Comparison of tensile strength data and
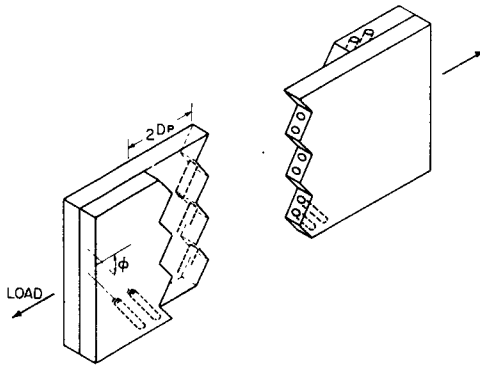$S = (130 \text{ MPa}) \cot \phi.$

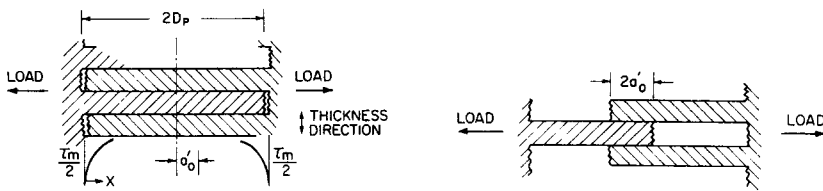*Figure 17. Typical fracture mode of a higher angle laminate.*

Figure 18. Delamination of plies during fracture. a) At the instant of fracture initiation. b) When the interlaminar shear force becomes negligible.

specimens that is associated with the increase in stress for transverse filament fracture in small $\alpha+\beta$ angle region (the small rise of segment BC in Fig. 10) does not occur.

Estimation of Fracture Toughness

The work of fracture associated with the delamination mechanism is an important contribution to the total fracture toughness in a composite material with some delamination in the course of fracture. Assume a laminate composite fracture that has plies pulled out as shown in Fig. 18a.

Because the fractured ply tip is free, and the clamping force on the separated layers is negligible close to the end of the lamina, the shear stress associated with the separation of the two halves is only significant when the total delamination size is longer than $2a_o'$. Figure 18b shows a case in which the shear stress is negligible. Assume the shear stress is highest at the root of the fractured lamina with a magnitude of one-half of the matrix shear strength τ_m, and decays exponentially, Fig. 18a. Since the source of the shear stress is the interlaminar friction, the percentage of bond contact does not affect the magnitude of the total resultant shear force. The shear stress is actually applied on both ends of the lamina. For simplicity, we will consider this situation to be equivalent to one single exponentially decaying shear stress with the highest magnitude of the matrix shear strength τ_m, i.e.:

$$\tau = \tau_m\, e^{-x/x_o}$$

where x_o is the distance, where τ_m is reduced by a factor of $1/e$. The energy consumed per unit of apparent (cross-sectional) crack surface is [7]:

$$R_{\text{pull-out}} = \frac{x_o\, \tau_m\cdot w\left(x_o - x_o\, e^{-D/x_o} - D\, e^{-D/x_o}\right)}{w\cdot t}\quad \text{(No. of interfaces)}$$

The energy needed to create new delamination surfaces, without regard to the above frictional energy, is [7]:

$$R_{\text{delamination surface}} = \frac{2\cdot D_p\cdot R_{if}(\%\text{contact})\,(\text{No. of interfaces})}{t}$$

The energy consumed in creating new surfaces is [2,9]:

$$R_{\text{main crack surface}} = \left[V_f R_f + (1-V_f)R_m + \frac{V_f s_c R_{if}}{d}\right]\left(1 - 2.4\frac{\tau_m}{\sigma_f}\tan\phi\right)$$

The work of fracture for composite laminates with the pull-out/delamination fracture mode is the total sum of the three:

$$R = R_{\text{pull-out}} + R_{\text{delamination surface}} + R_{\text{main crack surface}}$$

$$R = \frac{x_o \tau_m \left(x_o - x_o e^{-D/x_o} - D\, e^{-D/x_o} \right) (\text{No. of interfaces})}{t} +$$

$$\frac{2D_p \quad R_{if}\,(\%\ \text{contact})\,(\text{No. of interfaces})}{t} +$$

$$\left[V_f R_f + (1-V_f)\, R_m + \frac{V_f\, s_c\, R_{if}}{d} \right] \left[1 - 2.4 \left(\frac{\tau_m}{\sigma_f} \right) \tan \phi \right]$$

The application of this theory to our graphite/epoxy system has been examined. In our case, s_c is estimated from experimental data as $\simeq 0.09$ mm, $\sigma_f = 2.48$ GPa, no. of interfaces = 7, $V_f = 0.6$, $d = 6.9\ \mu$m and percent contact = 18 percent and 36 percent. After examining the fractographs we can choose $2a'_o = 7$ mm and assume $x_o = 1$ mm. D_p can be measured from each individual specimen. R_{if} is assumed to be equal to R_m. The properties of epoxy vary greatly due to its structure and curing cycle. Because of the lack of values for epoxy, we must make reasonable estimates: $R_m \simeq 2$ kJ/m² and $\tau_m \simeq 60$ MPa. (Notice that $\sigma_f/2\tau = 20.9$ while experimental values give $s_c/d = 13$.) We can also assume the value of $R_f V_f$ is very small and can be neglected.

A comparison of the calculated R values and the experimentally measured R values is shown in Fig. 19. In the plot, the ordinate is the measured R value and the abscissa represents the computed R value. Fairly good correlations between those two sets of values can be seen for 36 percent contact specimens and 18 percent specimens made from 1976 batch tape. The deviation of the data points from the theoretical 45° line is believed to be caused by the error in the assumptions of the constituent properties and individual variations of the specimen.

SYMBOLS

A Interlaminar fracture area.

a_o' One half maximum contact length for negligible drag force, Fig. 18.

D Effective average delamination length; $D = D_p - 2a'_o$.

D_p Average delamination length. d

d Diameter of the filament.
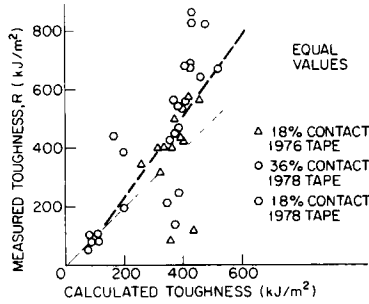
K Proportionality constant.

Figure 19. Comparison of measured and calculated toughness for 8-layer angle-ply laminates.

L	Maximum delamination length in Fig. 15.
R	Fracture toughness (energy consumed).
R_f	Surface energy of filament.
R_{if}	Difference in surface energies of filament and matrix.
R_m	Surface energy of matrix.
S	Strength.
s_c	Critical length of the filament.
t	Total thickness of laminate.
V_f	Volume fraction of filament.
w	Specimen width.
x	Distance from fracture in Fig. 18a.
x_o	Relaxation distance.
α	Average angle between fibers of all plies in a specimen and the loading direction.
β	Average angle between fibers of adjacent plies, taken for an entire specimen.
σ_f	Tensile strength of the filament.
τ_m	Interfacial shear strength.
ϕ	Angle between fibers of one ply and the loading direction.

ACKNOWLEDGEMENT

REFERENCES

1. W. T. Freeman and G. C. Kuebeler, "Mechanical and Physical Properties of Advanced Composites", ASTM STP 546 (1974), pp. 435–456.
2. T. U. Marston, A. G. Atkins and D. K. Felbeck, "Interfacial Fracture Energy and the Toughness of Composites", *Journal of Materials Science*, 9, (1974), pp. 447–455.

3. A. G. Atkins, "Interlaminar Bonding for High Toughness/High Strength Composites", *Journal of Materials Science*, 10, (1975), pp. 819–832.

4. K. Kendall, "Interfacial Cracking of Composite, Part 1 Interlaminar Shear and Tension", *Journal of Materials Science*, 11, (1976), pp. 638–644.

5. J. Cook and J. E. Gordon, "A Mechanism for the Control of Crack Propagation in All-Brittle Systems", Proc. of the Royal Society, A, 282, (1964), p. 508.

6. C. Gurney and J. Hunt, "Quasi-Static Crack Propagation", Proc. of the Royal Society, A, 297/8, (1967), p. 508.

7. L.-C. Jea, "Fracture Toughness of Graphite/Epoxy Composite Laminates Enhanced by the Intermittent-Interlaminar-Bonding Strength". Ph. D. dissertation, University of Michigan, (1979), pp. 62–89, 185–187.

8. L.-C. Jea and D. K. Felbeck, "Measurement of Fracture Toughness of Thin Graphite-Epoxy Composites in the Range 100 to 800 kJ/m^2", in preparation.

9. M. R. Piggott, "The Effect of Aspect Ratio on Toughness in Composite", *Journal of Materials Science*, 9, (1974), pp. 494–502.